LETTERS

Enhancing SIV-specific immunity *in vivo* by PD-1 blockade

Vijayakumar Velu[1,2]*, Kehmia Titanji[1,2]*, Baogong Zhu[3,4], Sajid Husain[1,2], Annette Pladevega[1,2], Lilin Lai[1,2], Thomas H. Vanderford[5], Lakshmi Chennareddi[1,2], Guido Silvestri[5], Gordon J. Freeman[3,4], Rafi Ahmed[1] & Rama Rao Amara[1,2]

Chronic immunodeficiency virus infections are characterized by dysfunctional cellular and humoral antiviral immune responses[1–3]. As such, immune modulatory therapies that enhance and/or restore the function of virus-specific immunity may protect from disease progression. Here we investigate the safety and immune restoration potential of blockade of the co-inhibitory receptor programmed death 1 (PD-1)[4,5] during chronic simian immunodeficiency virus (SIV) infection in macaques. We demonstrate that PD-1 blockade using an antibody to PD-1 is well tolerated and results in rapid expansion of virus-specific CD8 T cells with improved functional quality. This enhanced T-cell immunity was seen in the blood and also in the gut, a major reservoir of SIV infection. PD-1 blockade also resulted in proliferation of memory B cells and increases in SIV envelope-specific antibody. These improved immune responses were associated with significant reductions in plasma viral load and also prolonged the survival of SIV-infected macaques. Blockade was effective during the early (week 10) as well as late (~week 90) phases of chronic infection even under conditions of severe lymphopenia. These results demonstrate enhancement of both cellular and humoral immune responses during a pathogenic immunodeficiency virus infection by blocking a single inhibitory pathway and identify a novel therapeutic approach for control of human immunodeficiency virus infections.

Virus-specific T cells show varying degrees of functional impairment during chronic infections[6,7]. Although these T cells retain some antiviral functions, they are less polyfunctional compared with antiviral T cells seen in acute infections. This defect in T-cell function greatly contributes to the inability of the host to eliminate the persisting pathogen. The exhaustion of virus-specific T cells was first shown during persistent lymphocytic choriomeningitis virus (LCMV) infection of mice[8,9] and was quickly extended to other model systems including human immunodeficiency virus (HIV), hepatitis B virus (HBV) and hepatitis C virus (HCV) infections in humans[1,2,10]. The co-inhibitory receptor PD-1 has been shown to be highly expressed by exhausted LCMV-specific CD8 T cells and *in vivo* blockade of this pathway restores function in these cells[11]. PD-1 is also upregulated on HIV-1-specific[12–14] and SIV-specific[15,16] CD8 T cells and *in vitro* blockade of PD-1 enhances cytokine production and proliferative capacity of these cells. However, the importance of this PD-1 inhibitory pathway in regulating T-cell function during immunodeficiency virus infection *in vivo* is not known. Here, we use a SIV/macaque model to evaluate the effects of *in vivo* blockade of PD-1 on the safety and restoration of virus-specific cellular and humoral immunity during chronic immunodeficiency virus infections.

PD-1 blockade was performed using an antibody specific to human PD-1 that blocks the interaction between macaque PD-1 and its ligands (PDLs) *in vitro*[15]. Blockade was performed during the early (10 weeks) as well as late (~90 weeks) phases of chronic SIV infection. Nine macaques (five during the early phase and four during the late phase) received the anti-PD-1 antibody and five macaques (three during the early phase and two during the late phase) received an isotype control antibody (Synagis, anti-respiratory syncytial virus (RSV)-specific)[17].

PD-1 blockade during chronic SIV infection resulted in a rapid expansion of SIV-specific CD8 T cells in the blood of all macaques (Fig. 1a, b). We were able to study the CD8 T-cell responses to two immunodominant epitopes, Gag CM9 (ref. 18) and Tat SL8/TL8 (ref. 19), using major histocompatibility complex (MHC) I tetrameric complexes in seven of the anti-PD-1-antibody-treated and three of the control-antibody-treated macaques that expressed the Mamu A*01 histocompatibility molecule. Consistent with previous data[15], most (>98%) of the Gag-CM9 tetramer-specific CD8 T cells expressed PD-1 before blockade (data not shown). After PD-1 blockade, the Gag-CM9 tetramer-specific CD8 T cells expanded rapidly and peaked by 7–21 days. At the peak response, these levels were about 2.5–11-fold higher than their respective levels on day 0 ($P = 0.007$) and remained elevated until 28–45 days (Fig. 1b). Similar results were observed with blockade during the early as well as late phases of chronic SIV infection. A 3–4-fold increase in the frequency of Gag-specific interferon (IFN)-γ-positive CD8 T cells was also observed by day 14 after blockade in the two Mamu A*01-negative animals (RTd11 and RDb11), demonstrating that PD-1 blockade can enhance the frequency of virus-specific CD8 T cells that are restricted by non-Mamu A*01 alleles (data not shown). As expected, expansion of SIV-specific CD8 T cells was not observed in the control-antibody-treated macaques (Fig. 1).

PD-1 blockade was also associated with a significant increase in the frequency of virus-specific CD8 T cells that were undergoing active cell division *in vivo* with improved functional quality (Fig. 1b). Consistent with the rapid expansion of SIV-specific CD8 T cells, the frequency of Gag-CM9 tetramer-specific CD8 cells that co-expressed Ki67 (marker for proliferating cells) also increased as early as by day 7 after blockade ($P = 0.01$). Similarly, we observed an increase in the frequencies of Gag-CM9 tetramer-specific CD8 T cells co-expressing perforin and granzyme B (cytolytic potential; $P = 0.001$ and $P = 0.03$, respectively), CD28 (co-stimulation potential; $P = 0.001$), CD127 (proliferative potential; $P = 0.0003$)[20] and CCR7 (lymph-node homing potential; $P = 0.001$)[21]. We also observed a transient 1.5–2-fold increase in the

[1]Emory Vaccine Center, Emory University School of Medicine, Atlanta, Georgia 30322, USA. [2]Division of Microbiology and Immunology, Yerkes National Primate Research Center, Emory University, Atlanta, Georgia 30329, USA. [3]Department of Medical Oncology, Dana-Farber Cancer Institute, Boston, Massachusetts 02115, USA. [4]Department of Medicine, Harvard Medical School, Boston, Massachusetts 02115, USA. [5]University of Pennsylvania School of Medicine, University of Pennsylvania, Philadelphia, Pennsylvania 19104, USA. *These authors contributed equally to this work.

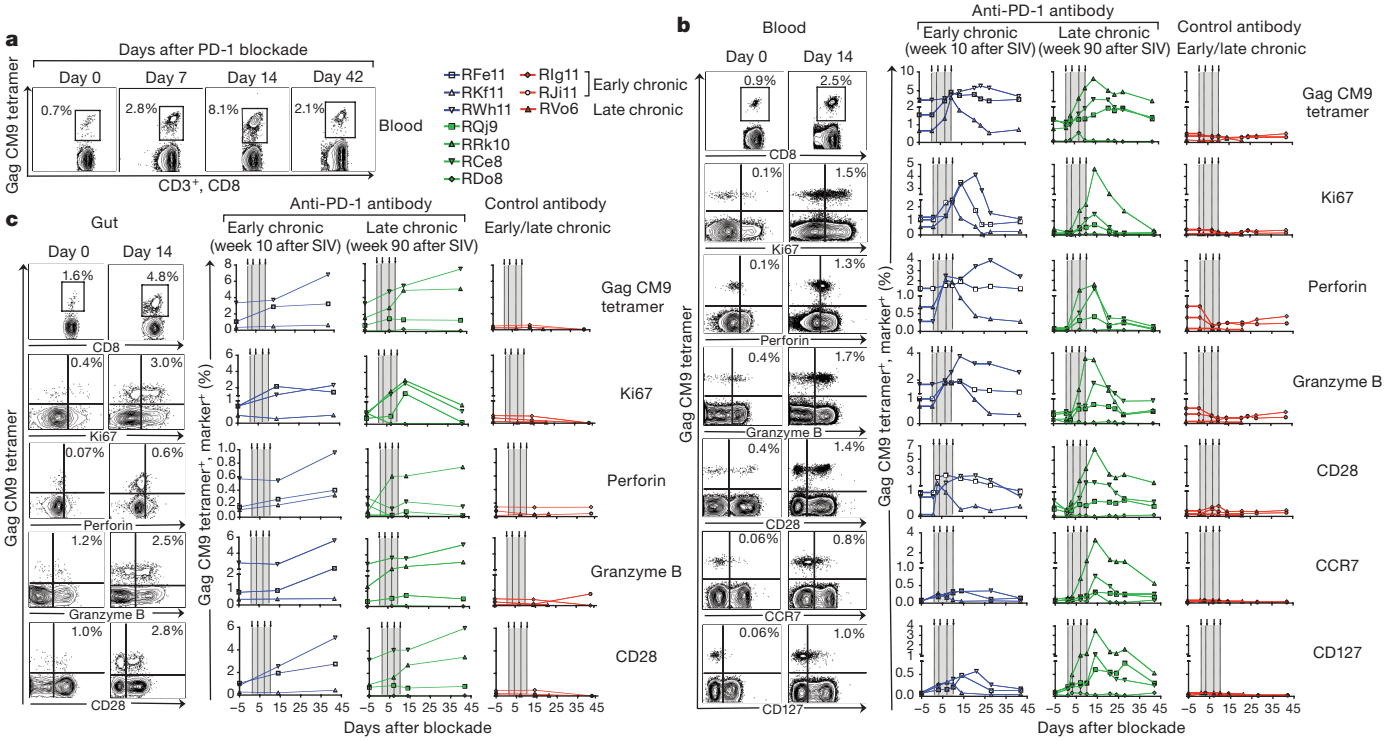

Figure 1 | *In vivo* PD-1 blockade during chronic SIV infection increases the Gag-CM9-specific CD8 T cells with improved functional quality in both blood and gut. **a**, Representative FACS plots for macaque RRk10. **b**, **c**, The magnitude and phenotype of Gag-CM9-tetramer-positive CD8 T cells in blood (**b**) and gut (colorectal mucosal tissue) (**c**). Representative FACS plots are shown on the left and summary for all Mamu A*01-positive animals is shown on the right. Numbers on the FACS plots represent the frequency of tetramer-positive cells as a per cent of total CD8 T cells. Arrows and vertical lines indicate anti-PD-1 antibody or control antibody treatment.

frequency of tetramer-negative and Ki67-positive CD8 T cells after blockade (data not shown). This could be due to expansion of CD8 T cells specific to other epitopes in Gag as well as other proteins of SIV, and other chronic viral infections in these animals. No significant enhancement was observed for these markers in the three control-antibody-treated macaques.

Notably, no expansion was observed for Tat-TL8-specific CD8 T cells after blockade (Supplementary Fig. 1a). This could be due to viral escape from recognition by Tat-TL8-specific CD8 T cells, as PD-1 blockade is known to result in expansion of T cells only when they simultaneously receive signals through T-cell receptor. To test this possibility, we sequenced the viral genomes present in the plasma just before the initiation of blockade from all three Mamu A*01-positive macaques that were infected with SIV251 and received the blocking antibody during the early phase of infection. Indeed, we found mutations in the viral genome corresponding to the Tat TL8 epitope region (Supplementary Fig. 1b). All these mutations either have been shown or predicted to reduce the binding of Tat SL8/TL8 peptide to Mamu A*01 MHC molecule and result in escape from recognition by the Tat-SL8/TL8-specific CD8 T cells[18,19]. These results suggest that *in vivo* blockade of PD-1 may not result in expansion of T cells that are specific to escape mutants of viral epitopes.

PD-1 blockade also resulted in expansion of Gag-CM9-specific CD8 T cells at the colorectal mucosal tissue (gut), a preferential site of SIV/HIV replication[22] (Fig. 1c). Expansion was not observed for two of the seven macaques, although expansion was evident for one of them in blood. In contrast to blood, the expansion in gut peaked much later by day 42 and ranged from 2- to 3-fold compared with their respective day 0 levels ($P = 0.003$). Similar to blood, the Gag-CM9 tetramer-specific cells that co-expressed Ki67 ($P = 0.01$), perforin ($P = 0.03$), granzyme B ($P = 0.01$) and CD28 ($P = 0.01$) also increased in the gut after blockade.

More importantly, PD-1 blockade also enhanced the functional quality of anti-viral CD8 T cells and resulted in the generation of polyfunctional cells capable of co-producing the cytokines IFN-γ, tumour-necrosis factor (TNF)-α and interleukin (IL)-2 (Fig. 2). On the day of initiation of PD-1 blockade during the late chronic phase of infection, the frequency of Gag-specific IFN-γ-positive cells was low and they failed to co-express TNF-α and IL-2 (Fig. 2a). However, after the blockade, the frequency of IFN-γ-positive cells increased in all four PD-1 antibody-treated macaques ($P = 0.03$) and they acquired the ability to co-express TNF-α and IL-2. The expansion of IFN-γ-positive cells peaked by 14–21 days and the peak levels were 2–10-fold higher than the respective day 0 levels. On day 21, about 16% of the total Gag-specific cells co-expressed all three cytokines, and about 30% co-expressed IFN-γ and TNF-α (Fig. 2b). This is in contrast to $<1\%$ of the total Gag-specific cells co-expressing all three cytokines ($P = 0.01$), and about 14% co-expressing IFN-γ and TNF-α on day 0 ($P = 0.04$). Similar results were also observed after blockade during the early chronic phase of infection (data not shown).

Recent studies have shown that chronic immunodeficiency virus infections are also associated with B-cell dysfunction[3] and very little is known about the role of PD-1 in regulating B-cell function/exhaustion. To understand the role of PD-1 in regulating B-cell function during chronic immunodeficiency virus infections, we characterized the B-cell responses after PD-1 blockade in SIV-infected macaques (Fig. 3). Analysis of PD-1 expression on different B-cell subsets before PD-1 blockade revealed preferential expression of PD-1 by memory B cells ($CD20^+CD27^+CD21^-$) compared to naive B cells ($CD20^+CD27^-CD21^+$; Fig. 3a, $P < 0.001$). *In vivo* blockade of PD-1 resulted in a 2–8-fold increase in the titre of SIV-specific binding antibody by day 28 after blockade ($P < 0.001$; Fig. 3b). To understand this further, we studied the proliferation of memory B cells in SIV-infected macaques that were treated simultaneously with anti-PD-1 antibody and anti-retroviral therapy and observed a significant increase in $Ki67^+$ (proliferating) memory, but not naive, B cells as early as day 3 (Fig. 3c). These results demonstrate that the PD-1–PDL pathway could have a role in regulating B-cell dysfunction during chronic SIV infection.

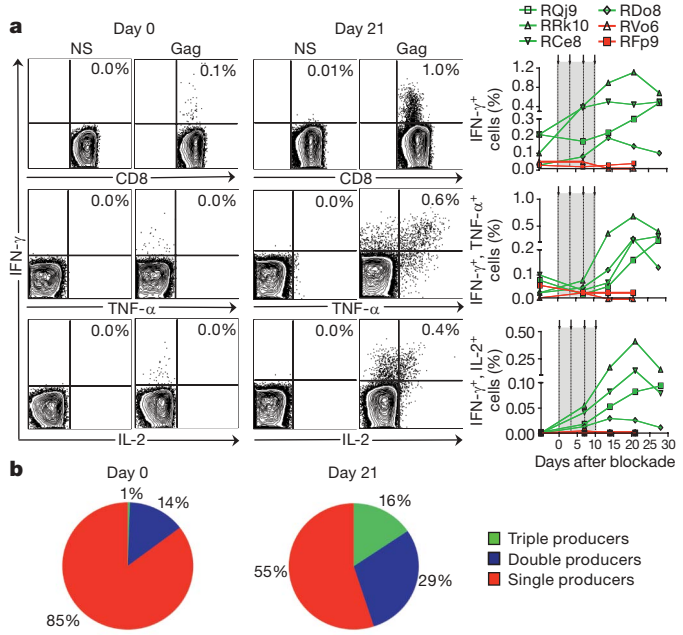

Figure 2 | *In vivo* PD-1 blockade during chronic SIV infection increases the polyfunctional virus-specific CD8 T cells. a, Frequency of Gag-specific cytokine-secreting CD8 T cells as a percentage of total CD8 T cells. Representative FACS plots are shown on the left and summary for the group is shown on the right. Arrows and vertical lines indicate anti-PD-1 antibody or control antibody treatment. Green lines represent anti-PD-1-antibody-treated macaques and red lines represent control-antibody-treated macaques. NS, no stimulation. **b**, Cytokine co-expression subsets expressed as a percentage of total cytokine-positive cells. Mean for the group is shown. Single producers, IFN-γ^+, TNF-α^+ or IL-2$^+$; double producers, IFN-γ^+TNF-α^+, IFN-γ^+IL-2$^+$ or IL-2$^+$TNF-α^+; triple producers, IFN-γ^+IL-2$^+$TNF-α^+.

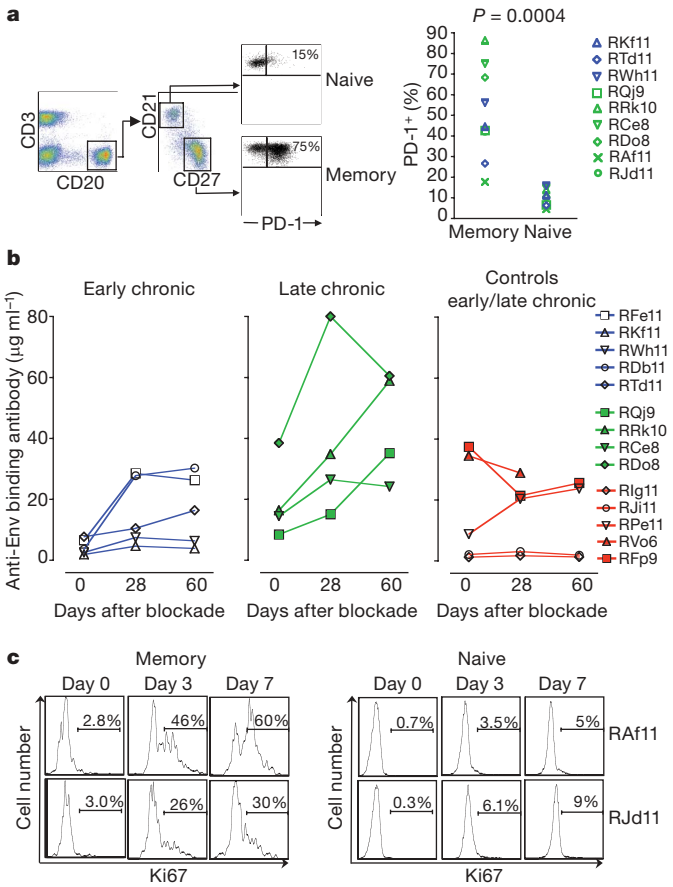

Figure 3 | *In vivo* PD-1 blockade during chronic SIV infection enhances SIV-specific humoral immunity. a, Expression of PD-1 on memory (CD20$^+$CD27$^+$CD21$^-$) and naive (CD20$^+$CD27$^-$CD21$^+$) B cells in blood after SIV infection and before *in vivo* PD-1 blockade. **b**, Titres of anti-SIV Env-binding antibody in serum after blockade. **c**, Ki67 expression (marker for proliferation) on memory and naive B cells after blockade. Numbers on the FACS plots represent Ki67-positive cells as a percentage of respective total naive/memory B cells. Macaques RAf11 and RJd11 were treated simultaneously with anti-PD-1 antibody and anti-retroviral therapy at 22 weeks after SIV infection.

Neutralization assays revealed a twofold increase in titres against the easily neutralizable laboratory-adapted SIV251 and no increase in titres against hard-to-neutralize wild-type SIV251 or SIV239 (data not shown). In two of the nine animals treated with anti-PD-1 antibody, we observed only a minimal (<2-fold) expansion of SIV-specific antibody after blockade. Notably, the frequency of total memory B cells in these two animals was lower (~40% of total B cells) compared with the remaining seven animals (60–90% of total B cells) before blockade (data not shown), indicating that the level of SIV-specific memory B cells before blockade may determine the level of expansion of SIV-specific antibody after blockade.

PD-1 blockade resulted in significant reductions in plasma viraemia ($P = 0.03$) and also prolonged the survival of SIV-infected macaques ($P = 0.001$; Fig. 4). In two of the five macaques treated with anti-PD-1 antibody during the early chronic phase, viral load declined by day 10 and persisted at or below this level until day 90 (Fig. 4a). In one macaque viral load declined transiently and in the remaining two macaques increased transiently and returned to pre-blockade levels. In contrast to the early chronic phase, all four macaques treated with the anti-PD-1 antibody during the late chronic phase showed a transient increase in viraemia by day 7, but rapidly reduced the virus load by day 21 to levels that were below their respective day 0 levels (Fig. 4b). However, the viral RNA levels returned to pre-blockade levels by day 43. As expected, no significant reductions in the plasma viral loads were observed in any of the five macaques treated with the control antibody (Fig. 4c). By 21–28 days after blockade, the viral RNA levels in the anti-PD-1-antibody-treated animals were 2–10-fold lower than their respective day 0 levels ($P = 0.03$; Fig. 4d). By day 150 after the blockade, four of the five macaques in the control group were killed owing to AIDS-related symptoms (for example loss of appetite, diarrhoea, weight loss), whereas all nine animals in the anti-PD-1-antibody-treated group had survived ($P = 0.001$; Fig. 4e).

The observed initial rise in plasma viraemia levels in all of the late-phase-treated and some of the early-phase-treated animals could be due to an increase in the frequency of activated CD4 T cells. To determine this, we measured the percentage of Ki67-positive total CD4 T cells as well as the frequency of SIV Gag-specific IFN-γ-producing CD4 T cells (preferential targets for virus replication[23]) after blockade (Supplementary Fig. 2). These analyses revealed a transient increase in the percentage of Ki67-positive CD4 T cells by day 7–14 after blockade ($P = 0.002$) and this increase was higher in animals treated during the late phase than early phase of infection ($P = 0.015$; Supplementary Fig. 2a). Similarly, an increase in the frequency of Gag-specific CD4 T cells was also observed, but only in animals treated during the late phase of infection (Supplementary Fig. 2b). No significant increases were observed for these activated CD4 T cells in the control-antibody-treated macaques. These results suggest that the activated CD4 T cells could have contributed to the observed initial rise in plasma viraemia levels after blockade.

It is to be noted that, before initiation of PD-1 blockade, the set point viral load in plasma and total CD4 T cells in blood and gut were similar between the anti-PD-1-antibody-treated and control-antibody-treated groups (Supplementary Fig. 3). However, the frequencies of Gag CM9$^+$ cells and Gag CM9$^+$ cells co-expressing perforin, granzyme B or CD28 were not similar between the two treatment groups before *in vivo* blockade (Fig. 1b). This raises the possibility that

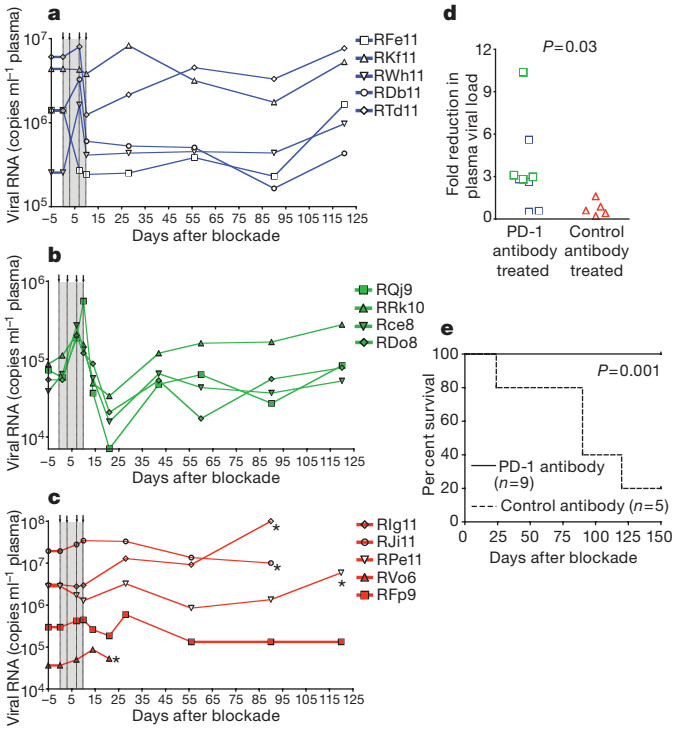

Figure 4 | *In vivo* PD-1 blockade reduces plasma viraemia and prolongs survival of SIV-infected macaques. **a**–**c**, Plasma viral load in macaques treated with anti-PD-1 antibody during the early chronic phase of infection (**a**), macaques treated with anti-PD-1 antibody during the late chronic phase of infection (**b**), and macaques treated with control antibody during the early/late chronic phase of SIV infection (**c**). An asterisk indicates death of animal. **d**, Fold reduction in plasma viral load between day 0 and day 28 (early chronic study) or day 0 and day 21 (late chronic study). The colour scheme is the same as that used in **a**–**c**. **e**, Survival of SIV-infected macaques after PD-1 blockade.

these differences could have contributed to the expansion of Gag $CM9^+$ cells after PD-1 blockade. To study the influence of the frequency of Gag $CM9^+$ cells before blockade on their expansion after blockade, we divided the anti-PD-1-antibody-treated group into two subgroups based on the frequency of Gag $CM9^+$ cells before initiation of blockade such that one group has similar levels and the other group has higher levels of Gag $CM9^+$ cells compared with the control-antibody-treated group. These subgroups were then analysed for expansion of Gag $CM9^+$ cells after blockade. Expansion of Gag $CM9^+$ cells was evident in both subgroups of animals after blockade of PD-1, irrespective of whether they were at low or high levels before blockade (Supplementary Fig. 4). Similar results were also observed with subgroup analyses based on the frequency of Gag $CM9^+$ cells co-expressing molecules associated with better T-cell function such as perforin, granzyme B, CCR7, CD127 or CD28 (Supplementary Fig. 4). However, we observed a trend towards better expansion of Gag $CM9^+CD28^+$ cells in animals with higher levels of Gag $CM9^+CD28^+$ cells before blockade, suggesting that CD28 expression may serve as a biomarker for predicting the outcome of *in vivo* PD-1 blockade.

To evaluate the safety of PD-1 blockade, we performed an extensive analysis of serum proteins, ions, lipids, liver and kidney enzymes, and complete blood count after blockade (Supplementary Tables 1 and 2). These analyses revealed no significant changes for all parameters tested between the anti-PD-1-antibody-treated and control-antibody-treated macaques (data not shown). Similarly, the levels of anti-nuclear antibodies (ANA) in serum (measure of autoimmunity) did not change significantly after treatment with anti-PD-1 antibody (Supplementary Fig. 5). In one macaque, the levels of ANA increased about 3-fold by day 10 after blockade, but returned to day 0 levels by day 56. These results demonstrate that anti-PD-1 antibody treatment during chronic SIV infection results in no observable toxicity. This is consistent with a recent study that demonstrated the safety of PD-1 blockade in patients with advanced haematological malignancies[24].

We studied the pharmacokinetics of the partially humanized anti-PD-1 antibody in serum after *in vivo* blockade. The titre of anti-PD-1 antibody rapidly declined between days 14 and 28 after blockade (Supplementary Fig. 6a) and coincided with macaques generating antibody response against the mouse immunoglobulin variable domains of anti-PD-1 antibody (Supplementary Fig. 6b). These results suggest that the use of completely humanized anti-PD-1 antibody may allow longer periods of treatment that may further enhance the efficacy of *in vivo* blockade.

Our results demonstrate that *in vivo* blockade of PD-1 during chronic SIV infection is safe and results in rapid expansion and restoration of SIV-specific polyfunctional CD8 T cells and enhanced B-cell responses. Expansion was observed with blockade performed during the early as well as late phases of chronic infection even under conditions of high levels of persisting viraemia and AIDS. Expansion was also observed at the colorectal mucosal tissue, a preferential site of SIV/HIV replication[22]. Importantly, PD-1 blockade resulted in a significant reduction of plasma viral load and also prolonged the survival of SIV-infected macaques. These results are highly significant considering the failure of blockade of a related co-inhibitory molecule CTLA-4 to expand virus-specific CD8 T cells and to reduce plasma viral load in SIV-infected macaques[25]. The therapeutic benefits of PD-1 blockade may be improved further by using combination therapy with anti-retrovirals and/or therapeutic vaccination.

METHODS SUMMARY

Study group. Fourteen Indian rhesus macaques (*Macaca mulatta*) infected with SIV were studied. Eight macaques were used for the early chronic phase and were infected intravenously with 200 50% tissue culture infectious dose ($TCID_{50}$) of SIV251. Six macaques were used for the late chronic phase, three were infected with SIV251 intrarectally and three were infected with SIV239 intravenously. All macaques, except RDb11, were negative for Mamu B08 and Mamu B17 alleles. RDb11 was positive for Mamu B17 allele. Macaques were housed at the Yerkes National Primate Research Center and were cared for under guidelines established by the Animal Welfare Act and the NIH 'Guide for the Care and Use of Laboratory Animals' using protocols approved by the Emory University IACUC.

***In vivo* antibody treatment.** Macaques were infused with either partially humanized mouse anti-human PD-1 antibody (clone EH12-1540)[26] or a control antibody (SYNAGIS). The anti-PD-1 antibody has mouse variable heavy chain domain linked to human IgG1 (mutated to reduce FcR and complement binding)[27] and mouse variable light chain domain linked to human κ. The clone EH12 binds to macaque PD-1 and blocks interactions between PD-1 and its ligands *in vitro*[15]. SYNAGIS is a humanized mouse monoclonal antibody (IgG1κ) specific to F protein of respiratory syncytial virus (Medimmune). Antibodies were administered intravenously at 3 mg kg^{-1} of body weight on days 0, 3, 7 and 10.

Immune responses. Peripheral blood mononuclear cells from blood and lymphocytes from rectal pinch biopsies were isolated as described previously[15]. Tetramer staining[28], intracellular cytokine production[28,29] and measurements of anti-SIV Env binding antibody[30] were performed as described previously.

Full Methods and any associated references are available in the online version of the paper at www.nature.com/nature.

Received 14 October; accepted 21 November 2008.
Published online 10 December 2008.

1. Letvin, N. L. & Walker, B. D. Immunopathogenesis and immunotherapy in AIDS virus infections. *Nature Med.* **9**, 861–866 (2003).
2. Pantaleo, G. & Koup, R. A. Correlates of immune protection in HIV-1 infection: what we know, what we don't know, what we should know. *Nature Med.* **10**, 806–810 (2004).
3. Moir, S. & Fauci, A. S. Pathogenic mechanisms of B-lymphocyte dysfunction in HIV disease. *J. Allergy Clin. Immunol.* **122**, 12–19 (2008).
4. Ishida, Y., Agata, Y., Shibahara, K. & Honjo, T. Induced expression of PD-1, a novel member of the immunoglobulin gene superfamily, upon programmed cell death. *EMBO J.* **11**, 3887–3895 (1992).
5. Sharpe, A. H., Wherry, E. J., Ahmed, R. & Freeman, G. J. The function of programmed cell death 1 and its ligands in regulating autoimmunity and infection. *Nature Immunol.* **8**, 239–245 (2007).

6. Wherry, E. J. *et al.* Molecular signature of $CD8^+$ T cell exhaustion during chronic viral infection. *Immunity* **27,** 670–684 (2007).
7. Klenerman, P. & Hill, A. T cells and viral persistence: lessons from diverse infections. *Nature Immunol.* **6,** 873–879 (2005).
8. Zajac, A. J. *et al.* Viral immune evasion due to persistence of activated T cells without effector function. *J. Exp. Med.* **188,** 2205–2213 (1998).
9. Gallimore, A. *et al.* Induction and exhaustion of lymphocytic choriomeningitis virus-specific cytotoxic T lymphocytes visualized using soluble tetrameric major histocompatibility complex class I-peptide complexes. *J. Exp. Med.* **187,** 1383–1393 (1998).
10. Rehermann, B. & Nascimbeni, M. Immunology of hepatitis B virus and hepatitis C virus infection. *Nature Rev. Immunol.* **5,** 215–229 (2005).
11. Barber, D. L. *et al.* Restoring function in exhausted CD8 T cells during chronic viral infection. *Nature* **439,** 682–687 (2006).
12. Petrovas, C. *et al.* PD-1 is a regulator of virus-specific $CD8^+$ T cell survival in HIV infection. *J. Exp. Med.* **203,** 2281–2292 (2006).
13. Day, C. L. *et al.* PD-1 expression on HIV-specific T cells is associated with T-cell exhaustion and disease progression. *Nature* **443,** 350–354 (2006).
14. Trautmann, L. *et al.* Upregulation of PD-1 expression on HIV-specific $CD8^+$ T cells leads to reversible immune dysfunction. *Nature Med.* **12,** 1198–1202 (2006).
15. Velu, V. *et al.* Elevated expression levels of inhibitory receptor programmed death 1 on simian immunodeficiency virus-specific CD8 T cells during chronic infection but not after vaccination. *J. Virol.* **81,** 5819–5828 (2007).
16. Petrovas, C. *et al.* SIV-specific $CD8^+$ T-cells express high levels of PD1 and cytokines but have impaired proliferative capacity in acute and chronic SIVmac251 infection. *Blood* **110,** 928–936 (2007).
17. Malley, R. *et al.* Reduction of respiratory syncytial virus (RSV) in tracheal aspirates in intubated infants by use of humanized monoclonal antibody to RSV F protein. *J. Infect. Dis.* **178,** 1555–1561 (1998).
18. Allen, T. M. *et al.* Characterization of the peptide binding motif of a rhesus MHC class I molecule (Mamu-A*01) that binds an immunodominant CTL epitope from simian immunodeficiency virus. *J. Immunol.* **160,** 6062–6071 (1998).
19. Allen, T. M. *et al.* Tat-specific cytotoxic T lymphocytes select for SIV escape variants during resolution of primary viraemia. *Nature* **407,** 386–390 (2000).
20. Kaech, S. M. *et al.* Selective expression of the interleukin 7 receptor identifies effector CD8 T cells that give rise to long-lived memory cells. *Nature Immunol.* **4,** 1191–1198 (2003).
21. Sallusto, F., Lenig, D., Forster, R., Lipp, M. & Lanzavecchia, A. Two subsets of memory T lymphocytes with distinct homing potentials and effector functions. *Nature* **401,** 708–712 (1999).
22. Pierson, T., McArthur, J. & Siliciano, R. F. Reservoirs for HIV-1: mechanisms for viral persistence in the presence of antiviral immune responses and antiretroviral therapy. *Annu. Rev. Immunol.* **18,** 665–708 (2000).
23. Douek, D. C. *et al.* HIV preferentially infects HIV-specific $CD4^+$ T cells. *Nature* **417,** 95–98 (2002).
24. Berger, R. *et al.* Phase I safety and pharmacokinetic study of CT-011, a humanized antibody interacting with PD-1, in patients with advanced hematologic malignancies. *Clin. Cancer Res.* **14,** 3044–3051 (2008).
25. Cecchinato, V. *et al.* Immune activation driven by CTLA-4 blockade augments viral replication at mucosal sites in simian immunodeficiency virus infection. *J. Immunol.* **180,** 5439–5447 (2008).
26. Dorfman, D. M., Brown, J. A., Shahsafaei, A. & Freeman, G. J. Programmed death-1 (PD-1) is a marker of germinal center-associated T cells and angioimmunoblastic T-cell lymphoma. *Am. J. Surg. Pathol.* **30,** 802–810 (2006).
27. Xu, D. *et al. In vitro* characterization of five humanized OKT3 effector function variant antibodies. *Cell. Immunol.* **200,** 16–26 (2000).
28. Amara, R. R. *et al.* Control of a mucosal challenge and prevention of AIDS by a multiprotein DNA/MVA vaccine. *Science* **292,** 69–74 (2001).
29. Kannanganat, S., Ibegbu, C., Chennareddi, L., Robinson, H. L. & Amara, R. R. Multiple-cytokine-producing antiviral CD4 T cells are functionally superior to single-cytokine-producing cells. *J. Virol.* **81,** 8468–8476 (2007).
30. Lai, L. *et al.* GM-CSF DNA: an adjuvant for higher avidity IgG, rectal IgA, and increased protection against the acute phase of a SHIV-89.6P challenge by a DNA/MVA immunodeficiency virus vaccine. *Virology* **369,** 153–167 (2007).

Supplementary Information is linked to the online version of the paper at www.nature.com/nature.

Acknowledgements The authors thank J. D. Altman for provision of Gag CM9 and Tat SL8 tetramers, H. Drake-Perrow for administrative support, and D. Watkins and Wisconsin National Primate Research Center Genotyping Service for Mamu typing of animals. The authors also thank the Yerkes Division of Research Resources for pathology support, Emory CFAR virology core for viral load assays and the NIH AIDS Research and Reference Reagent Program for the provision of peptides. This work was supported by the National Institutes of Health/National Institute of Allergy and Infectious Diseases grants R01 AI057029, R01 AI071852, R01 AI074417 to R.R.A.; the Foundation for the NIH through the Grand Challenges in Global Health initiative P51 RR00165 to R.A., G.J.F. and R.R.A.; Yerkes National Primate Research Center base grant P51 RR00165; Emory CFAR grant P30 AI050409; and R24 RR16038 to David I. Watkins.

Author Contributions V.V. and K.T. contributed to the design of experiments, conducted analyses on T-cell responses, and contributed to manuscript preparation; S.H. performed analyses on T-cell phenotyping. T.H.V. performed analyses on viral escape. L.L. and A.P. performed analyses on humoral responses; L.C. performed the statistical analysis; G.S. supervised the analyses on viral escape and contributed to manuscript preparation; B.Z. and G.J.F. developed and provided the anti-human PD-1 blocking antibody, and contributed to the design of experiments and manuscript preparation. R.A. contributed to the concept, design of experiments and manuscript preparation. R.R.A. supervised the entire project, designed and coordinated the experiments, and contributed to manuscript preparation.

Author Information Sequencing data related to the Tat SL8/TL8 epitope region have been deposited in GenBank (accession numbers FJ268664–FJ268704). Reprints and permissions information is available at www.nature.com/reprints. The authors declare competing financial interests: details accompany the full-text HTML version of the paper at www.nature.com/nature. Correspondence and requests for materials should be addressed to R.R.A. (ramara@emory.edu).

METHODS

B-cell responses. A total of 100 μl of blood was surface stained with antibodies to CD3 (clone SP34-2, BD Biosciences), CD20 (2H7, e-Biosciences), CD21 (B-ly4, Becton Dickson) CD27 (M-T2712, Becton Dickson) and PD-1 (clone EH-12), each conjugated to a different fluorochrome. Cells were lysed and fixed with FACS lysing solution, and permeabilized using FACS perm (BD Biosciences) according to the manufacturer's instructions. Cells were then stained for intracellular Ki67 using an anti-Ki67 antibody conjugated to phycoerythrin (clone B56, Becton Dickson). After staining, cells were washed and acquired using LSRII (BD Biosciences), and analysed using FlowJo software.

Titres of anti-PD-1 antibody and monkey antibody response against anti-PD-1 antibody in serum. To measure the levels of anti-PD-1 antibody, plates were coated with goat anti-mouse immunoglobulin (pre-absorbed to human immunoglobulin, Southern Biotech), blocked and incubated with different dilutions of serum to capture the PD-1 antibody. Bound antibody was detected using anti-mouse IgG conjugated to HRP (pre-absorbed to human immunoglobulin, Southern Biotech). Known amounts of PD-1 antibody captured in the same manner were used to generate a standard curve. To measure the levels of monkey antibody response against the anti-PD-1 antibody, plates were coated with anti-PD-1 antibody (5 $\mu g\,ml^{-1}$), blocked and incubated with different dilutions of serum to capture monkey antibody against the anti-PD-1 antibody. Bound antibody was detected using anti-human λ-chain-specific antibody conjugated to HRP (Southern Biotech). This detection antibody does not bind to the PD-1 antibody because only the constant regions of the heavy and light chains were humanized and the constant region of the light chain is κ. The amount of captured monkey immunoglobulin was estimated using a standard curve that consisted of known amounts of purified macaque immunoglobulin that had been captured using anti-macaque immunoglobulin.

Quantification of SIV copy number. SIV copy number was determined using a quantitative real-time PCR as previously described[28]. All specimens were extracted and amplified in duplicates, with the mean result reported.

Amplification and sequencing of the Tat TL8 epitope. A 350-nucleotide fragment including Tat TL8 epitope was amplified by limiting dilution RT–PCR. Viral RNA was extracted using the QIAamp Viral RNA mini kit (Qiagen) from plasma. vRNA was reverse transcribed with the SIVmac239-specific primer Tat-RT3 (5′-TGGGGATAATTTTACACAAGGC-3′) and Superscript III (Invitrogen) using the manufacturer's protocol. The resultant cDNA was diluted and copy number was determined empirically in our nested PCR protocol. Limiting dilution, nested PCR was performed at ~0.2 copies per reaction using the Expand HiFi PCR kit (Roche Applied Sciences) with outer primers Tat-F1 (5′-GATGAATGGGTAGTGGAGGTTCTGG-3′) and Tat-R2 (5′-CCCAAGTATCCCTATTCTTGGTTGCAC-3′), and inner primers Tat-F3 (5′-TGATCCTCGCTTGCTAACTG-3′) and Tat-R3 (5′-AGCAAGATGGCGATAAGCAG-3′). The first round reactions were cycled using the following programme: 94 °C for 1 min, followed by 10 cycles of 94 °C for 30 s, 55 °C for 30 s, and 68 °C for 1 min, followed by 25 more cycles identical to the first ten but for the addition of 5 s to the extension time at every cycle, followed by a final extension at 68 °C for 7 min. The second round reactions were cycled using the following programme: 94 °C for 1 min, followed by 35 cycles of 94 °C for 30 s, 53 °C for 30 s, and 68 °C for 1 min, followed by a final extension at 68 °C for 7 min. After clean-up with ExoSap-IT (USB Corporation), PCR products were sequenced directly using the inner primers on an automated sequencer at The Children's Hospital of Philadelphia's Napcore sequencing facility. Contigs were assembled using Sequencher 4.8 (Gene Codes Corporation). Amplicons containing nucleotides with double chromatogram peaks were excluded.

Statistical analyses. Linear mixed effects models were used to determine differences in blood chemistry and complete blood count values between anti-PD-1-antibody-treated and control-antibody-treated animals. The Bonferroni method was used to adjust P values for multiple tests. A paired t-test was used for comparison of immune responses before and after PD-1 blockade. Log-transformed data were used when the data were not normal, but log-normal. A Wilcoxon rank-sum test was used to compare the fold reductions in viral loads between the groups. A Mantel–Haenszel log rank test was used to compare the survival curves between the groups. Statistical analyses were performed using S-PLUS 8.0. A two-sided $P < 0.05$ was considered statistically significant.